Iterative tomography: error projection along ellipses and lines

Marta Jo Woodward

Introduction

The goal of tomography is the reconstruction of a function from a set of line integrals through that function. Thus, for the cross-hole experiment shown in Figure 1, a tomographic inversion seeks to transform the 961 first break traveltimes, t_j, corresponding to the 961 source-receiver pairs, j, into the medium slowness function, w—via the system of equations

$$t_j = \int w \, dl_j(w) \; ; \quad j = 1, 2, \ldots 961. \tag{1}$$

Here $l_j(w)$ describes the ray optics raypath for the j-th source-receiver pair. When line integrals exist for all possible paths through a function, the relation between the integrals and the function may be interpreted as a Radon transform—the inverse of which is known to be unique (Menke, 1984). When the experimental geometry is incomplete, as in Figure 1, the solution contains a null space, limiting the resolution of the inversion and giving rise to artifacts. The resolution may be enhanced by constraining the solution with information distinct from the first break traveltimes—by filling the null space with additional information.

The literature contains many examples of enhanced reconstructions, where the extra information ranges from the angle of arrival at three-component geophones (Del Pino, 1985), to statistical estimates of properties of the ensemble of realizable functions (Hanson, 1983). This paper first reviews the basic ART algorithm and then describes two modifications of the iterative method as applied to the simple experiment of Figure 1. The first modification supplements the traveltime data with diffraction information present in the wavefield immediately following the first break; the second does not add to the available information but rather smooths it in a manner consistent with the experimental geometry. Both methods differ from the ART algorithm in projecting iterative slowness corrections back along elliptical regions and/or broad lines instead of narrow raypaths.

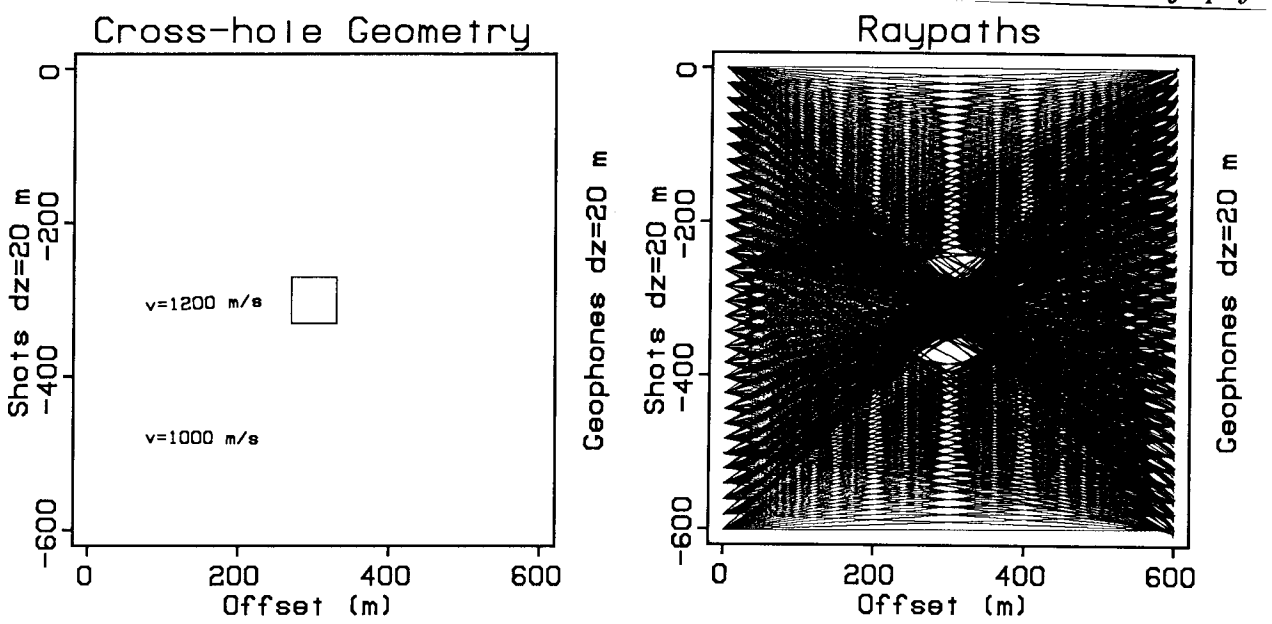

Figure 1: A cross-hole tomography experiment with 31 shots and 31 receivers evenly spaced every 20 m in holes 600 m deep and 600 m apart. The central anomaly is a 60 m by 60 m square of 1200 m/s material on a background of 1000 m/s material.

ART1: Projecting Slowness Errors Along Narrow Lines

Figure 2 shows the fifth iteration in an iterative solution to the seismic tomography problem posed in Figure 1. The solution was generated using a version of ART (Algebraic Reconstruction Technique) modified to include refraction, developed and described by Al-Yahya in SEP-42 (and henceforward referred to as ART1). The algorithm consists of an iterative solution of the equations

$$t_j = \sum_i w_i l_i \; ; \quad j = 1, 2, \ldots 961, \tag{2}$$

where the continuous line integrals of Equation 1 have been approximated through discretization: both of the slowness function w into 961 cells, w_i, and of the raypath $l_j(w)$ into line segments, l_i. The method is implemented in four steps. First, an initial slowness model, $\hat{w}_i$, is guessed (for this application the guess was the background velocity, 1000 m/s). Second, rays are traced through the guessed slowness model, yielding estimated traveltime data, $\hat{t}_j$, along estimated raypaths, l_i, and linear equations

$$\Delta t_j = \sum_i \Delta w_i l_i \; ; \quad j = 1, 2, \ldots 961. \tag{3}$$

Here $\Delta t_j = t_j - \hat{t}_j$ and $\Delta w_i = w_i - \hat{w}_i$. Third, for each source-receiver traveltime, the underdetermined Δt_j equation is solved by minimizing the minimax norm $L^\infty = \sum_i (\Delta w_i)^\infty$, yielding the slowness corrections

$$\Delta w_i = \frac{\Delta t_j}{\sum_i l_i} \; ; \quad j = 1, 2, \ldots 961. \tag{4}$$

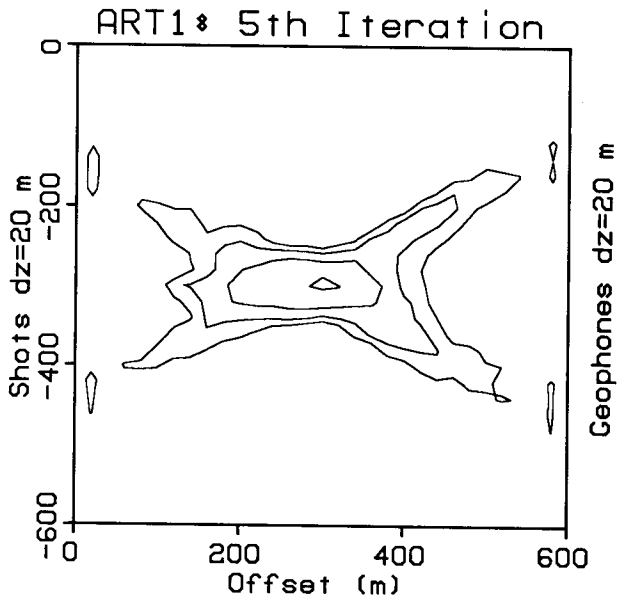

Figure 2: ART1: the fifth iteration in an ART solution to the tomography problem posed in Figure 1. The outermost contour corresponds to 1010 m/s. The contours increase towards a maximum of 1040 m/s at the center in 10 m/s increments.

Note that the corrections for all the cells along a single raypath are identical and that a single error is projected back along a single trajectory. Fourth, after slowness corrections are calculated for each cell for all traversing raypaths, the median Δw_i for each cell is selected to construct a new slowness model guess, and the entire process is repeated.

Even though the number of measurements (961 traveltimes) equals the number of unknowns (961 slowness cells) for the experiment of Figure 1, the cross-hole geometry limits the line integrals through the cells and consequently the linkage between the cells; the problem is underdetermined and the solution exhibits a loss of resolution. Distinctive, geometry-dependent artifacts are apparent, particularly in the horizontal direction.

ART2: Projecting Slowness Errors Along Ellipses and Lines

The algorithm described above is based solely on first break traveltimes; it discards the bulk of the wavefield information contained in the seismograms recorded at each receiver. In his classic paper on migration, Hagedoorn makes an observation which suggests a method for incorporating part of this information in the inversion process (Hagedoorn, 1954). Two figures illustrating bandlimited wave propagation through a *homogeneous* medium are reproduced from his paper in Figure 3. For the source wavelet shown in the upper part of the figure, Hagedoorn notes that: "Analogous to the principle of Huygens-Fresnel, an energy quantum from the source S in fig. 2 [lower part of Figure 3] can contribute to the first compression received in R if its trajectory

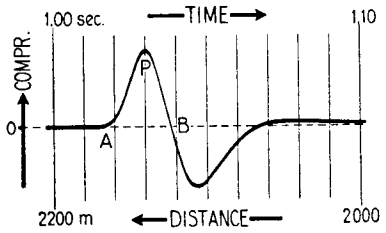

Fig. 1. A simple type of waveform from a seismic shot.

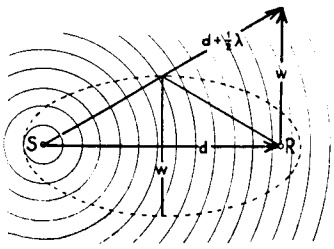

$$d^2 + w^2 = (d + \tfrac{1}{2}\lambda)^2 = d^2 + d\lambda + \tfrac{1}{4}\lambda^2$$

$$w \approx \sqrt{d\lambda}$$

distance: d	from	500	to 10000	m.
velocity: V	„	1000	„ 6000	m/sec.
frequency: n	„	10	„ 100	cycles/sec.
wavelength: $\lambda = V/n$	„	10	„ 600	m.
width: w	„	70	„ 2500	m.

Fig. 2. The width of a beam between shotpoint and receiver for the practical magnitudes of distance and frequency.

Figure 3: Two figures borrowed from Hagedoorn (1954) which demonstrate that the first pulse of a bandlimited signal propagating through a homogeneous medium is influenced by an elliptical region separating the source and receiver.

does not exceed the minimum path by more than a half wavelength, corresponding roughly to the distance from A to B in fig. 1 [upper part of Figure 3]," (ibid.). Thus the region influencing the first pulse recorded for any source-receiver pair in a homogeneous medium is described by an ellipse of width $\sim \sqrt{d\lambda}$, where d is the source-receiver distance and λ is the dominant source wavelength. This reasoning implies that anomalous zones within a homogeneous region may be detected by comparison of the first pulse of a cross-hole seismogram with a reference source wavelet; the presence or absence of interference effects in the first pulse for any source-receiver pair can be interpreted as an indication of the inhomogeneity or homogeneity of the intervening elliptical region. (For this argument the ellipse widths are fixed at $\sqrt{d\lambda}$. A more general formulation of the relation would require source deconvolution prior to examination of the seismograms; the ellipse widths would then be made dependent on the distance between the first and second spikes on the deconvolved traces.)

These ideas are applied to the simple cross-hole problem of Figure 1 in Figure 4. Panel (a) describes the interaction of a 40 Hz source wavelet with the experiment's single central velocity anomaly, as interpreted by Hagedoorn's model. For a source-receiver pair such as A-B, the elliptical region influencing the first pulse is homogeneous and the model predicts the absence of interference effects from the first recorded pulse; for a source-receiver pair such as A-C, the elliptical region intersects the anomaly and the model predicts the presence of interference effects. Panel (b) shows a synthetic time section generated by placing a 40 Hz source at shotpoint A of

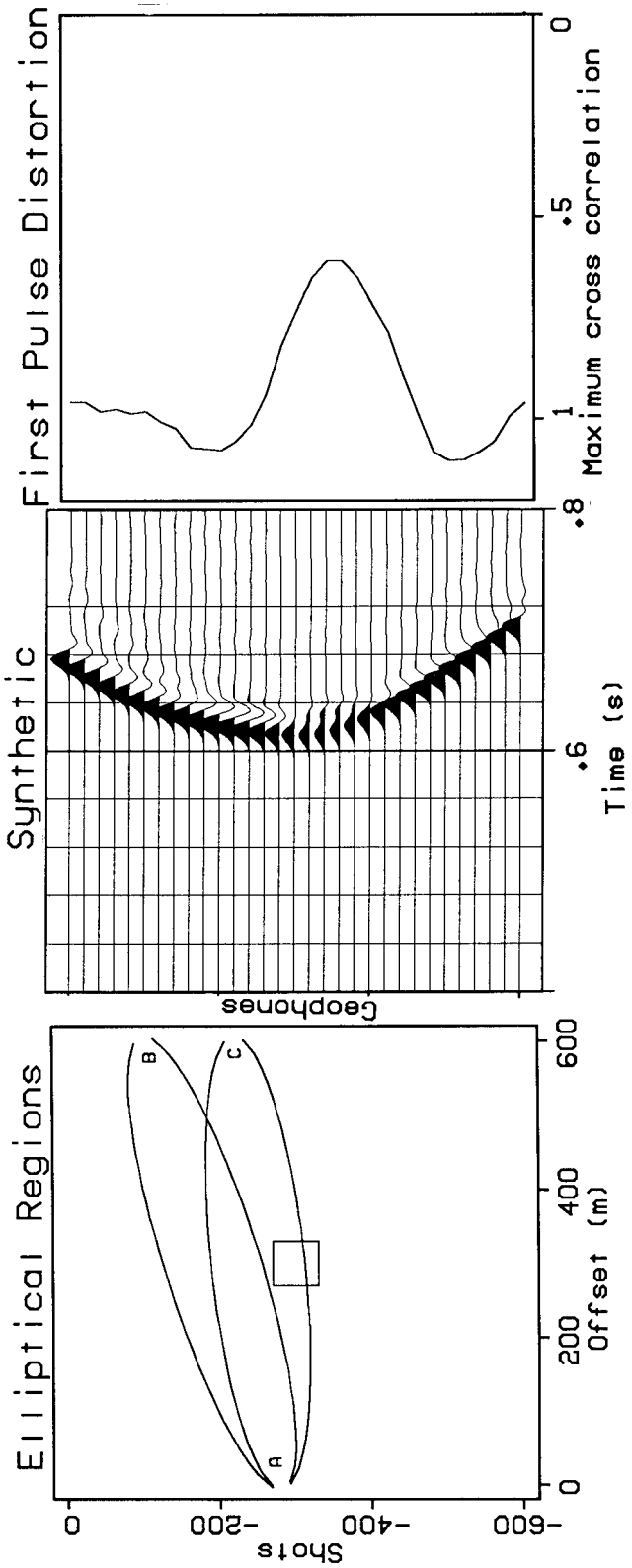

Figure 4: (a): The elliptical regions which influence the first pulse arriving at receivers B and C from source A, assuming a bandlimited wavelet with a dominant frequency of 40 Hz and the experiment of Figure 1. (b): A synthetic time section generated by placing a 40 Hz source at shotpoint A. (c): A smoothed plot of the maximum cross correlation of the first pulse after the first break on each trace of Panel (b) with the first pulse of the original source.

Panel (a). Panel (c) shows a smoothed plot of the maximum cross correlation of the first pulse of the original source with the first pulse after the first break of each trace in Panel (b). Hagedoorn's model predicts the data correctly; diffraction effects appear when the central anomaly impinges on the elliptical region of wave propagation connecting the source-receiver pairs.

These relations suggest a scheme for improving the tomographic inversion of the simple experiment of Figure 1, based upon the inclusion of information contained in the first pulse following the first break. The information may be incorporated by modification of step three of the ART1 algorithm described above. When interference effects from reflections or diffractions are absent from the first pulse—when the elliptical region is known to be uniform—slowness corrections are projected back over an elliptical region. By linking the cells within the ellipse this step forces homogeneity of the region in the final solution. When interference effects are present—when the elliptical region is known to be nonuniform—slowness corrections are projected back over the usual narrow raypath of ART1. Figure 5 shows the fifth iteration of the ART2 algorithm, modified according to this scheme with the assumption of a 40 Hz source; slowness corrections were redistributed along both lines and ellipses. Horizontal resolution has been improved and the distinctive artifacts have been removed. By projecting errors back over an ellipse, the algorithm effectively deduces absent line integrals; more cells are linked in more ways by the broad ellipses than by the narrow raypaths.

ART3: Projecting Slowness Errors Along Broad Lines

Two factors are responsible for ART2's success in the above example. First, because the experiment was synthetic, detection of distortion in the first pulse was trivial. For real data this operation would have been much more difficult, if not impossible. Second, the simple geometry permitted projection of slowness errors back along either straight ellipses, or straight and/or curved lines. Regions influencing the first pulse after the first break for more complicated media are illustrated in Figure 6: the upper panel diagrams reflection; the lower panel diagrams transmission through layered media. For these cases it is more difficult to determine the path for redistribution of slowness errors, but not impossible.

Because of these difficulties, it is interesting to consider the consistent projection of slowness errors back along broad lines instead of either narrow raypaths or combinations of narrow raypaths and ellipses. Figure 7 shows the fifth iteration in a third version of the ART algorithm, modified according to this scheme; error corrections were projected back along broad (120 m) raypaths for every source-receiver pair. While the method has decreased the information in the inversion and consequently reduced resolution in both the vertical and horizontal directions, it has successfully removed the x-shaped artifacts which dominate Figure 2. By smoothing in a direction perpendicular to the raypaths, ART3 has low-pass filtered the sharp truncations in the spatial frequency

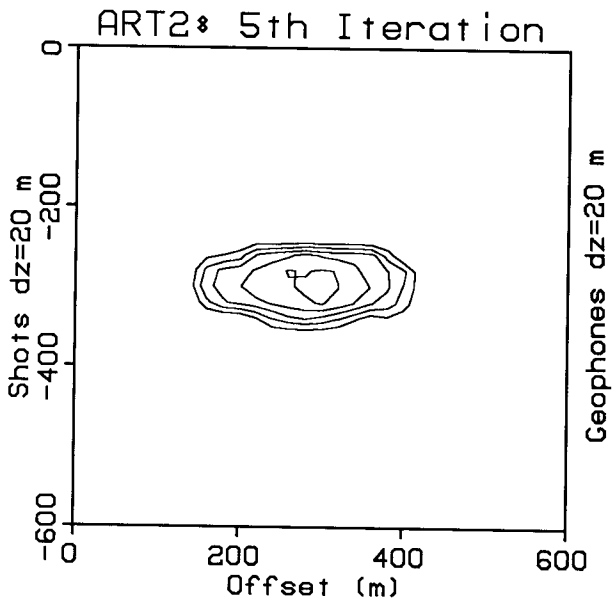

Figure 5: ART2: the fifth iteration in an ART solution to the tomography problem posed in Figure 1, modified to project slowness errors back over an elliptical region when the first pulse generated by a 40 Hz source was free of interference effects, and over a narrow raypath when the first pulse showed interference effects. The outermost contour corresponds to a velocity of 1010 m/s. The contours increase towards the center to a maximum of 1050 m/s in 10 m/s increments.

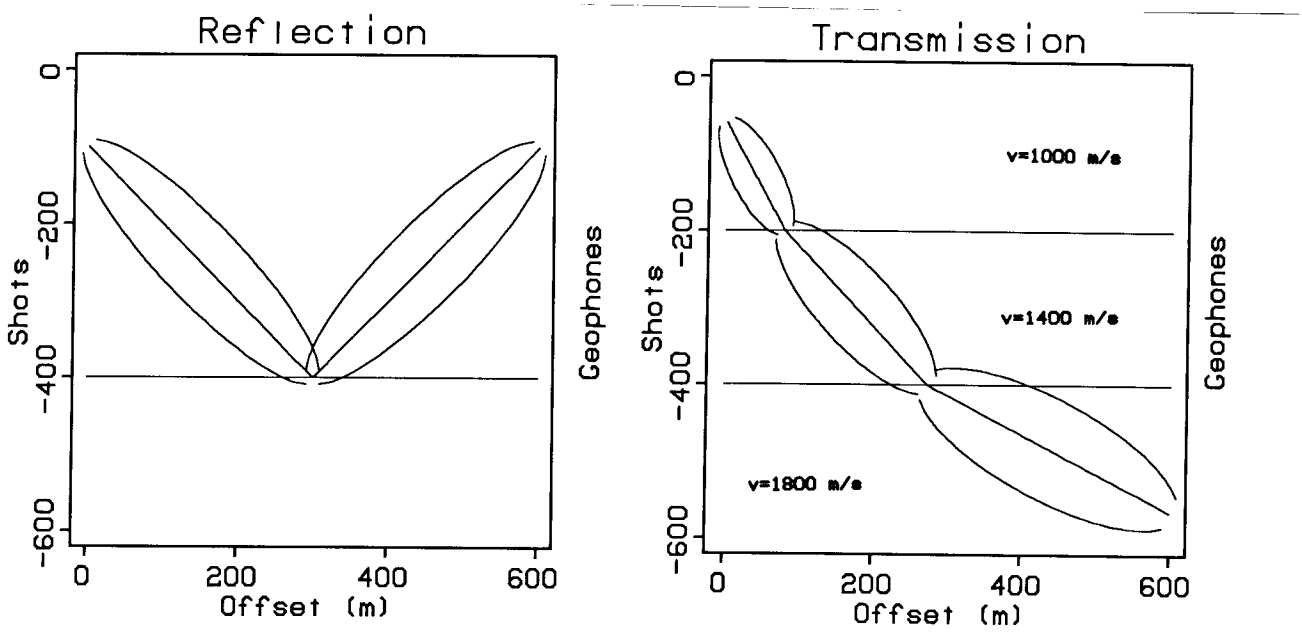

Figure 6: (a): The elliptical regions affecting the first pulse of a reflected wave, adapted from Hagedoorn (1954). (b): The elliptical regions affecting the first pulse of a wave transmitted through layered media.

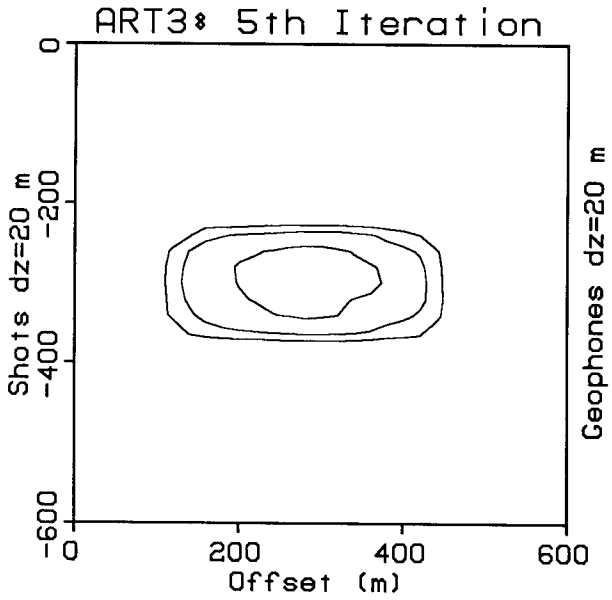

Figure 7: ART3: the fifth iteration in an ART solution to the tomography problem of Figure 1, modified to project slowness errors back along broad (120 m) raypaths between every source-receiver pair. The outermost contour corresponds to a velocity of 1010 m/s. The contours increase towards the center to a maximum of 1030 m/s in 10 m/s increments.

domain which probably caused the artifacts in the first place (Hanson, 1982). Significantly, this third scheme is compatible with the idea of picking peaks instead of first breaks. Where tomographic inversion is performed on picked peak rather than first break times, the first pulse of an event is automatically assumed to be undistorted and the intervening medium smoothly varying around the raypath.

Summary

Because of practical limitations on experimental geometry, geophysical tomography problems are generally underdetermined; their traveltime inversions demonstrate poor resolution and geometry-dependent artifacts. Resolution may be enhanced and artifacts removed by constraining the null space of the solution with extra information or a priori assumptions. Two methods are described above for improving the basic iterative ART solution to the simple cross-hole problem of Figure 1. The first modification is based on Hagedoorn's observation that the first pulse of a bandlimited signal propagating through a homogeneous medium interacts with an elliptical region separating source and receiver. Iterative slowness corrections are projected back over an elliptical region when interference effects from reflections and diffractions are absent from the first pulse—when the elliptical region is known to be uniform; the corrections are projected back over a narrow raypath when interference effects are present—when the elliptical region is known

to be nonuniform. This method adds information to the tomographic solution, both improving horizontal resolution and removing artifacts. The second modification is based on recognition of the fact that inversion artifacts arise from sharp edges in experimental geometries. Iterative slowness corrections are consistently projected back over broadened raypaths, smoothing the inversion result along the natural lines of the problem. This method adds a priori information to the tomographic solution, removing artifacts at the expense of horizontal and vertical resolution. The ability of the two modifications to improve inversion results for geometries more complicated than Figure 1 remains to be studied.

Acknowledgements

I wish to thank Kamal Al-Yahya and Stew Levin for many illuminating consultations.

References

Al-Yahya, K., 1985, An iterative solution to seismic tomography, SEP-42.

Del Pino, E. A., 1985, Seismic wave polarization applied to geophysical tomography, Stanford Rock Physics Project.

Hagedoorn, J. G., 1954, A process of seismic reflection interpretation: Geophysical Prospecting, v. 2, p. 85-127.

Hanson, K. M., 1982, CT reconstruction from limited projection angles, Proc. Application of Photo-Optical Instrumentation in Medicine X, New Orleans, Proc. SPIE 374, p. 166-173.

Hanson, K. M., and Wecksung, G. W., 1983, Bayesian approach to limited-angle reconstruction in computed tomography: Journal of the Optical Society of America (preprint).

Menke, W., 1984, The resolving power of cross-borehole tomography: Geophysical Research Letters, v. 11, no. 2, p. 105-108.

搬迁

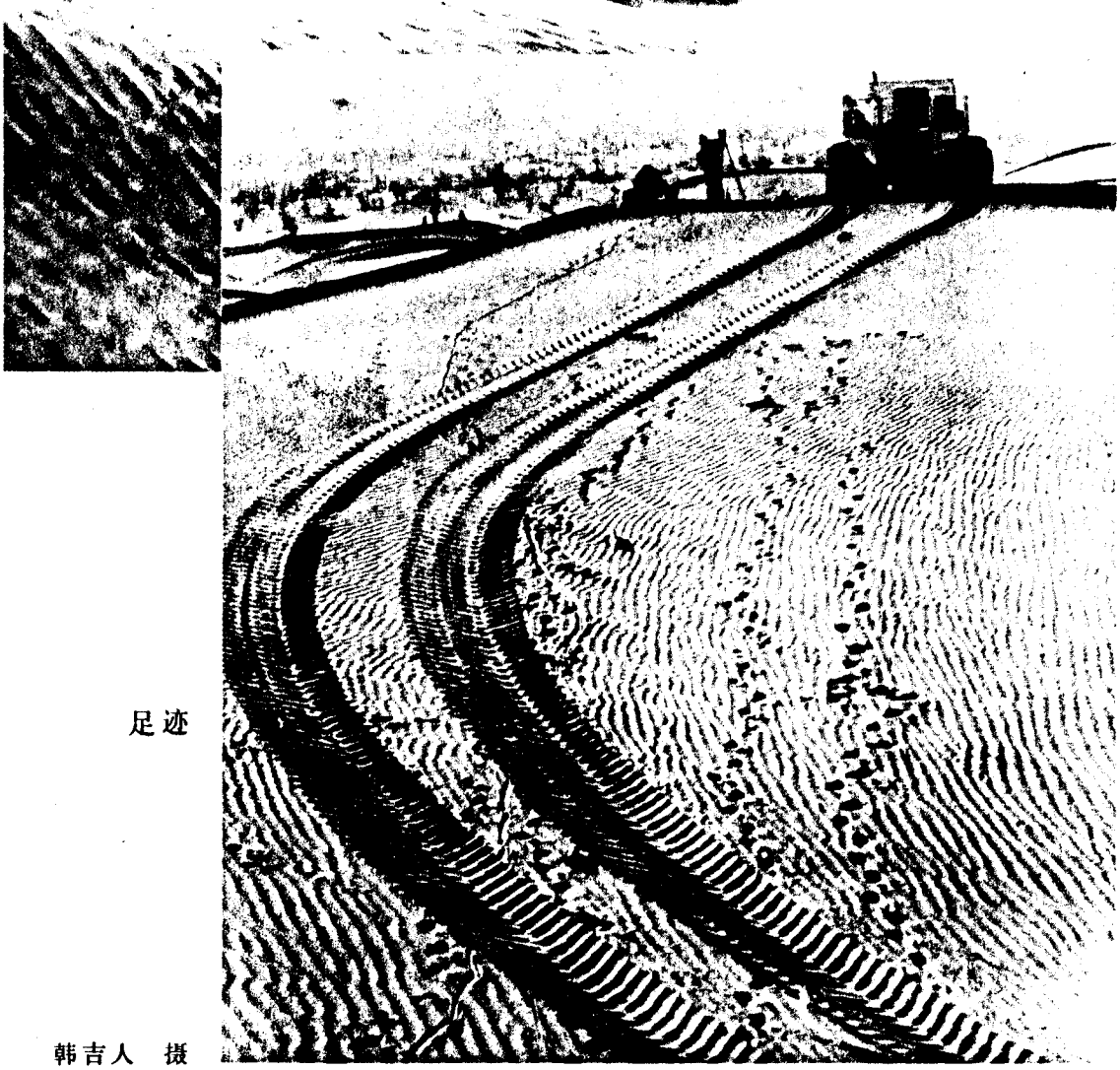

足迹

韩吉人　摄